

0.001–0.005 M) in 5 mL volumetric flasks were incubated in a thermostated bath. After the desired temperature was reached, 15  $\mu$ L of the substrate (final concentration ca. 0.02 M) were injected into the solutions. When the reactions were completed (as indicated by the disappearance of the yellow color of the bromine), or shortly before it, 0.1 mL of saturated sodium thiosulfate methanolic solution and 0.1 mL of a 10% solution of sodium bicarbonate in MeOH were injected to quench the reaction. The “dibromo” to “bromomethoxy” ratio was determined by GC analysis. In order to ensure that the same product ratio was also obtained in the kinetic experiments that were performed with less concentrated solutions, samples were also taken from the latter, concentrated, and GC analyzed. The results obtained showed both types of experiments to yield identical results.

**Solvolytic Reactions.** To a test tube containing 10 mL of 0.2 M AgNO<sub>3</sub> methanolic solution, 0.4 g (0.0016 mol) of **2a** were added. The test tube was immersed in a bath at 50 °C for 5 days. The reaction mixture was filtered and the filtrate was washed several times with ether. The combined organic phases were washed twice with water and twice again with salt-saturated water. Evaporation of the ether gave a yellow liquid from which 3-methylene-1-bromocyclobutanecarbonitrile [<sup>1</sup>H NMR  $\delta$  3.35–3.7 (m, 4 H), 4.9–5.17 (t, 2 H); MS, *m/z* 174, 172, 147, 145, 92, 65] (unstable compound, decomposes at room temperature) and 3-methoxy-3-methyl-1-bromocyclobutanecarbonitrile (**2b'**) [<sup>1</sup>H NMR  $\delta$  1.51 (s, 3 H), 3.18, 3.1, 2.78, 2.74 (AB q, 4 H), 3.17 (s, 3 H); MS, *m/z* 206, 204, 174, 172, 125, 110] (satisfactory C, H, N, Br analysis was obtained) were separated by preparative gas chromatography. GC yields of these and the unidentified products are given in Scheme I.

**Acknowledgment.** The authors are grateful to Dr. F. Frolow of the Weizmann institute for performing the X-ray analysis and

to Profs. M. Sprecher, E. M. Kosower, and J. K. Kochi for helpful discussions.

## Appendix

Steady-state assumption for I gives

$$[I] = \frac{k_1[S][Br_2] + k_2'[S][Br_3^-]}{k(I)_a[Br^-] + k(I)_b}$$

Substituting this expression for I in eq 6 and using the equation  $[Br_3^-] = K[Br_2][Br^-]$  gives

$$Q - \frac{k(I)_a[Br^-]}{k(I)_b} = \frac{k_{cat}[Br^-](k(I)_a[Br^-] + k(I)_b)}{k(I)_b(k_1 + k_2'K[Br^-])}$$

Since  $k_2'K = k_2K - k_{cat}$  one obtains

$$Q - \frac{k(I)_a[Br^-]}{k(I)_b} = \frac{k_{cat}[Br^-](k(I)_a[Br^-] + k(I)_b)}{k(I)_b(k_1 + k_2K[Br^-] - k_{cat}[Br^-])}$$

from which eq 7 is easily derived.

**Registry No.** 1, 16955-35-4; **1a**, 30628-80-9; **1b**, 109151-11-3; **2**, 694-25-7; **2a**, 109151-12-4; **2b**, 109151-13-5; **2b'**, 109151-14-6; **3**, 23745-75-7; **3a**, 109151-15-7; **3c**, 109151-16-8; **4**, 30494-27-0; **4b** (isomer 1), 109151-17-9; **4b** (isomer 2), 109151-18-0; **6**, 109151-10-2; **Br<sub>3</sub><sup>-</sup>**, 14522-80-6; **Br<sup>-</sup>**, 24959-67-9; methanol, 67-56-1; 3-bromocyclobutyl cation, 109151-09-9; 1-bromo-3-methylenecyclobutylcarbonitrile, 109151-19-1.

## Consequences of $\pi/\sigma$ Interaction in Bishomoanthraquinones and Their Dimethylene Derivatives. A Structural and PE Spectroscopic Study

Rolf Gleiter,\*† Walter Dobler,† Emanuel Vogel,\*‡ Stefan Böhm,‡ and Johann Lex†

Contribution from the Institut für Organische Chemie der Universität Heidelberg, D-6900 Heidelberg, West Germany, and Institut für Organische Chemie der Universität Köln, D-5000 Köln 41, West Germany. Received December 30, 1986

**Abstract:** The syntheses of *syn*- and *anti*-7,14-dihydro-7,14-dimethylene-1,6:8,13-bismethano[14]annulene (**1** and **2**) and of the corresponding 17,17,18,18-tetramethyl compounds (**3** and **4**) starting from *syn*- and *anti*-bishomoanthraquinones (**6** and **7**), respectively, are described. The molecular structures of **6** and **7** have been determined by X-ray analysis. For **6** four independent molecules are found in the unit cell whereas for **7** all molecules are related by symmetry. A great similarity between the molecular parameters of **6** and **7** is observed. As anticipated, both compounds exhibit pronounced bond alternation in the hexatriene systems. The He I photoelectron (PE) spectra of **1**–**6** are reported. Assignment of the bands below 12 eV is based on semiempirical calculations (MINDO/3). A comparison of the PE spectra of **1** and **2** with the spectrum of their planar congener, dibenzo-*p*-quinodimethane (**5**), indicates considerable  $\pi/\sigma$  interaction in the bridged species. A comparison between **1** and **3** and **2** and **4**, respectively, provides evidence for unusual large Koopmans' defects. Very strong  $\pi/\sigma$  interactions in **6** and **7** are inferred by comparing the widths of the group of the first six PE bands of these compounds (1.6 eV) with the width of the first peak of **8** (0.8 eV) which contains six transitions.

In planar  $\pi$  systems like ethylene or benzene, symmetry can be used to discriminate between  $\pi$  and  $\sigma$  electrons. If the symmetry is reduced and  $\pi$  and  $\sigma$  systems are no longer orthogonal, mutual interaction occurs. The size of this interaction depends on several factors, e.g., the overlap integral between  $\pi$  and  $\sigma$  system and the energy difference of the corresponding basis orbital energies. In organic chemistry two effects, i.e., hyperconjugation<sup>1</sup> and the through-bond interaction,<sup>2</sup> are due to a sizable conjugation between a planar  $\pi$  system and an adjacent  $\sigma$  framework. In both

cases a 2p orbital of a planar  $\pi$  system can interact with an adjacent  $\sigma$  bond as indicated in A (hyperconjugation) or B (through-bond interaction). The electronic nature of the  $\pi$  systems

(1) Mulliken, R. S. *J. Chem. Phys.* **1939**, *7*, 339. Mulliken, R. S.; Rieke, C. A.; Brown, W. G. *J. Am. Chem. Soc.* **1941**, *63*, 41. Baker, J. W. *Hyperconjugation*; Oxford, 1952. Coulson, C. A.; Crawford, V. A. *J. Chem. Soc.* **1953**, 2052.

(2) Hoffmann, R.; Imamura, A.; Hehre, W. J. *J. Am. Chem. Soc.* **1968**, *90*, 1499. Heilbronner, E.; Schmelzer, A. *Helv. Chim. Acta* **1975**, *58*, 936. Reviews: Hoffmann, R. *Acc. Chem. Res.* **1971**, *4*, 1. Gleiter, R. *Angew. Chem.* **1974**, *86*, 770; *Angew. Chem., Int. Ed. Engl.* **1974**, *13*, 696. Padon-Row, M. N. *Acc. Chem. Res.* **1982**, *15*, 245.

\*Institut für Organische Chemie der Universität Heidelberg.

†Institut für Organische Chemie der Universität Köln.

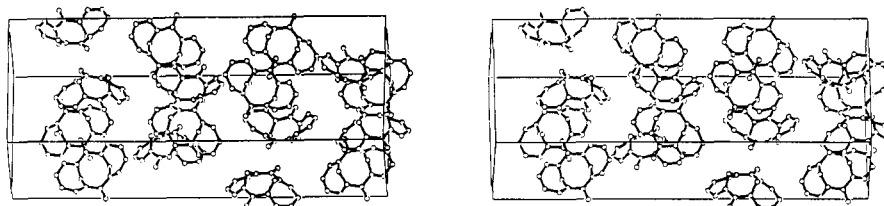


Figure 1. Stereoscopic view of the molecular conformation and packing of 6.

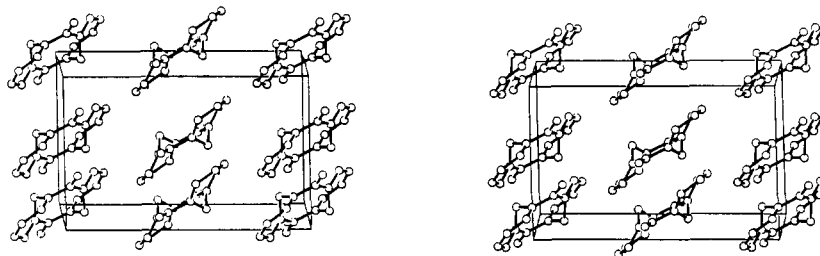


Figure 2. Stereoscopic view of the molecular conformation and packing of 7.

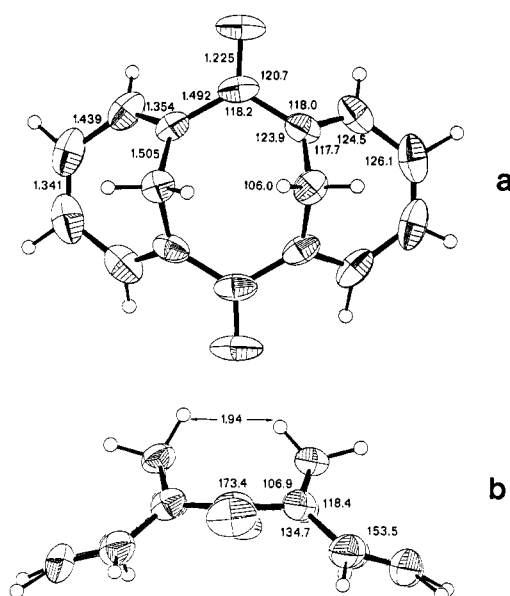
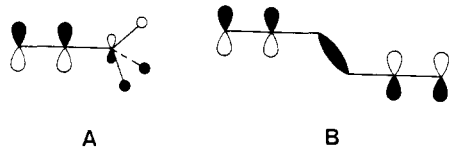


Figure 3. (a) Average bond lengths and bond angles of 6. (b) Side view of 6 with dihedral angles between least-squares planes as well as the contact distances between the two inner hydrogen atoms of the bridges.

(filled or unfilled orbitals) determines whether the  $\pi/\sigma$  interaction stabilizes or destabilizes the molecule.



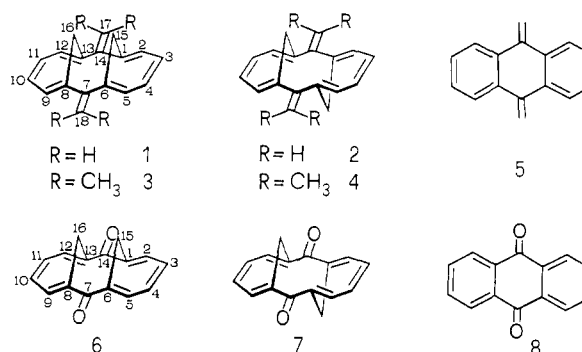
A  $\pi/\sigma$  interaction different from that just described is encountered in molecules in which the  $\sigma$  frame of the  $\pi$  system is bent, such as  $\Delta^{1,3}$ -bicyclo[1.1.0]butene,<sup>3</sup> *syn*-sesquinorbornene,<sup>4</sup> and [5]paracyclophane.<sup>5</sup> Several model calculations on the

compounds mentioned<sup>6-8</sup> suggest a considerable mixing of the  $\pi$  and  $\sigma$  MOs.



The recent synthesis of *syn*- and *anti*-1,6:8,13-bismethano[14]annulene and some of its derivatives<sup>9</sup> makes it possible to study the effects of  $\pi/\sigma$  interaction in nonplanar  $\pi$  systems by comparing the properties of these compounds with those of their planar congeners.

In this paper we report the He I $\alpha$  photoelectron (PE) spectra of *syn*- and *anti*-7,14-dihydro-7,14-dimethylene-1,6:8,13-bismethano[14]annulene (1 and 2), the corresponding 17,17,18,18-tetramethyl compounds (3 and 4), and the 7,14-dioxo compounds (6 and 7).<sup>9d</sup> The latter can be considered as bishomoanthraquinones while 1 and 2 can be viewed as bishomodibenzo-*p*-quinodimethanes. Since our spectroscopic evaluations are based on the different geometrical parameters of the planar (5, 8) and nonplanar (1-4, 6, 7) species, we also report the X-ray data of 6 and 7. Compounds 1-4 have been prepared from 6 and 7, respectively, using standard procedures (see Experimental Section).



(3) Szeimies, G.; Harnisch, J.; Baumgärtel, O. *J. Am. Chem. Soc.* **1977**, *99*, 5183.

(4) Bartlett, P. D.; Blakeney, A. J.; Combs, G. L.; Galloy, J.; Roof, A. A. M.; Subramanyam, R.; Watson, W. H.; Winter, W. J.; Wu, C. In *Stereochemistry and Reactivity of Systems containing  $\pi$  Electrons*; Watson, W. H., Ed.; Verlag Chemie Int.: Deerfield Beach, FL, 1983.

(5) Allinger, N. L.; Sprague, J. T.; Liljefors, T. *J. Am. Chem. Soc.* **1974**, *96*, 5100. Jenneskens, L. W.; de Kanter, F. J. J.; Kraakman, P. A.; Turkenburg, L. A. M.; Koolhaas, W. E.; de Wolf, W. H.; Bickelhaupt, F.; Tobe, Y.; Kakiuchi, K.; Odaira, Y. *Ibid.* **1985**, *107*, 3716.

(6) Wagner, H.-U.; Szeimies, G.; Chandrasekhar, J.; Schleyer, P. v. R.; Pople, J. A.; Binkley, J. S. *J. Am. Chem. Soc.* **1978**, *100*, 1210.

(7) Spanget-Larsen, J.; Gleiter, R. *Tetrahedron* **1983**, *39*, 3345. Houk, K. N.; Rondan, N. G.; Brown, F. K.; Jorgensen, W. L.; Madura, J. D.; Spellmeyer, D. C. *J. Am. Chem. Soc.* **1983**, *105*, 5980 and references therein.

(8) Schmidt, H.; Schweig, A.; Thiel, W.; Jones, M., Jr. *Chem. Ber.* **1978**, *111*, 1958. Gleiter, R.; Hopf, H.; Eckert-Maksic, M.; Noble, K.-L. *Ibid.* **1980**, *113*, 3401.

(9) (a) Vogel, E.; Biskup, M.; Vogel, A.; Haberland, U.; Eimer, J. *Angew. Chem.* **1966**, *78*, 642; *Angew. Chem., Int. Ed. Engl.* **1966**, *5*, 603. (b) Vogel, E.; Sombroek, J.; Wagemann, W. *Angew. Chem.* **1975**, *87*, 591; *Angew. Chem., Int. Ed. Engl.* **1975**, *14*, 564. (c) For a review, see: Vogel, E. *Pure Appl. Chem.* **1982**, *54*, 1015. (d) Vogel, E.; Böhm, S.; Hedwig, A.; Hergarten, B. O.; Lex, J.; Uschmann, J.; Gleiter, R. *Angew. Chem.* **1986**, *98*, 1001; *Angew. Chem., Int. Ed. Engl.* **1986**, *25*, 1000.

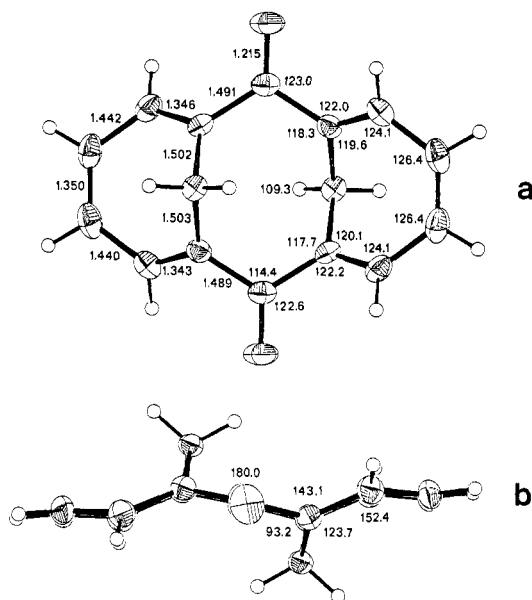


**Figure 4.** (a) Bond lengths and bond angles of 7. (b) Side view of 7 with dihedral angles between least-squares planes.

### Structural Studies on the Bishomoanthraquinones (6 and 7)

X-ray crystallographic investigations reveal that 6 has four independent molecules in the unit cell while in 7 all molecules are related by symmetry (see Figure 1 and 2). This difference can be ascribed to the difference in the geometry of the perimeters of 6 and 7. In the anti compound 7, the perimeter is puckered, but it possesses a grossly planar shape, allowing the molecules to stack in layers. By contrast, the syn compound features a noticeably bent perimeter, which leads to a complex arrangement in the crystal devoid of symmetry.

In Figure 3a the average bond lengths and bond angles of 6 are presented. Figure 3b gives a side view of 6 with dihedral angles between least-squares planes, as well as the contact distances between the two inner bridge H atoms. In Figure 4 the corresponding data for 7 are shown. Tables containing the atomic parameters, bond lengths, bond angles, and torsional angles of 6 and 7 are provided as supplementary material. The molecular parameters of both compounds are quite similar. We notice a pronounced bond alternation in the hexatriene systems of both molecules. The bond lengths and outer bond angles of the cycloheptatriene structural moieties of 6 and 7 are nearly identical. The only larger difference is found in the angles of the central eight-membered ring. This can be traced back to the close proximity of the two CH<sub>2</sub> bridges in 6. The distance between the two internal hydrogen atoms of the bridging CH<sub>2</sub> groups is found to be 1.94 Å. Due to this repulsion of the CH<sub>2</sub> groups in 6 the angle C(1)–C(15)–C(6), measuring 106.0°, is smaller than that found in 7 (109.3°). All the other angles in the central eight-membered ring of 6 are enlarged as compared to 7.

A comparison of the torsional angles shows a very close similarity of 6 and 7 with respect to the maximal values (45.0 and 44.9°) as well as the average values (27.2 and 25.0°).

Both compounds can be looked upon as two cycloheptatriene units connected by two carbonyl groups. The distance between the two olefinic termini, e.g., C(1) and C(6), is found to be 2.405 Å. This value is close to that found in *cis,cis,cis*-cyclonona-1,4,7-triene (2.46 Å)<sup>10</sup> for which a sizeable homoconjugation has been deduced.<sup>11</sup> A comparison of the molecular parameters of 6 and 7 with those of anthraquinone<sup>12</sup> shows a marked difference in so far as the bond lengths in the two benzene rings of the latter

(10) Roth, W. R.; Bang, W. P.; Göbel, P.; Sass, R. L.; Turner, R. B.; Yu, A. P. *J. Am. Chem. Soc.* **1964**, *86*, 3178. Jackson, R. B.; Sheib, W. E. *Ibid.* **1967**, *89*, 2539.

(11) Bischof, P.; Gleiter, R.; Heilbronner, E. *Helv. Chim. Acta* **1970**, *53*, 1425.

(12) Prakash, A. *Acta Crystallogr.* **1967**, *22*, 439.

**Table I.** Comparison between the Vertical Ionization Energies,  $I_{v,j}$ , and the Calculated Orbital Energies,  $\epsilon_j$ , of 1–4<sup>a</sup>

compd	band	$I_{v,j}$	assignment	$-\epsilon_j$ (MINDO/3)
1	1	7.9	14a <sub>1</sub>	7.60
	2	8.15	12b <sub>2</sub>	7.95
	3	8.7	10b <sub>1</sub>	8.45
	4	9.0	8a <sub>2</sub>	8.92
	5	9.5	9b <sub>1</sub>	9.69
	6	9.96	7a <sub>2</sub>	10.15
	7	10.5	13a <sub>1</sub>	10.64
2	1	7.45	13b <sub>u</sub>	7.58
	2	8.44	13a <sub>g</sub>	8.09
	3	8.7	9b <sub>g</sub>	8.71
	4	9.0	9a <sub>u</sub>	8.76
	5	9.8	9b <sub>g</sub>	9.95
	6	9.9	12b <sub>u</sub>	10.09
	7	10.6	11b <sub>u</sub>	10.81
3	1	7.5	17a <sub>1</sub>	7.92
	2	7.9	15b <sub>2</sub>	7.97
	3	8.3	13b <sub>1</sub>	8.61
	4	8.7	11a <sub>2</sub>	9.31
	5		12b <sub>1</sub>	9.14
	6	9.3	10a <sub>2</sub>	9.78
	7	10.2	16a <sub>1</sub>	9.80
4	1	7.0	16b <sub>u</sub>	7.70
	2	7.9	16a <sub>g</sub>	8.54
	3	8.3	12a <sub>u</sub>	8.57
	4	8.8	12b <sub>g</sub>	9.01
	5	9.4	11b <sub>g</sub>	9.52
	6	9.6	15b <sub>u</sub>	9.36
	7	10.3	14b <sub>u</sub>	10.79

<sup>a</sup> The calculations were carried out with the MINDO/3 method. All values in eV.

compound vary only between 1.381 and 1.401 Å.

### PE Spectra of 1–4

The PE spectra of 1–4 are shown in Figure 5. The PE spectrum of 1 shows a broad peak (bands 1 and 2) at 8 eV followed by five bands below 11 eV. The PE spectrum of the anti isomer 2 is different in so far as only four peaks and one shoulder are present below 11 eV. The second and fourth peaks are broader than the first and third ones. The relative areas suggest to assign two transitions to the second and fourth peaks while only one transition to the first and third peaks as well as to the shoulder at 10.6 eV is assigned.

The PE spectrum of 3 is rather complex in that the first bands overlap strongly. The comparison between the PE spectra of 2 and 4 shows that bands 2 and 3 are split in the spectrum of 4 while bands 5 and 6 are still close in energy. The recorded ionization energies for 1–4 are listed in Table I.

To interpret the PE spectra, we assume that the recorded vertical ionization energy ( $I_{v,j}$ ) can be set equal to the negative value of the orbital energy ( $-\epsilon_j$ ) calculated by current SCF procedures.

$$I_{v,j} = -\epsilon_j$$

In this approximation (Koopmans' theorem<sup>13</sup>) it is a basic tenet that the wave functions which describe the ground state of a molecule properly are also valid for its various ionic states. Although this is a very crude approximation since it supposes a cancellation of relaxation and correlation effects, it has been shown in many investigations that for large organic systems it holds quite well in the outer valence region.

In Table I we have compared the calculated orbital energies derived by the MINDO/3 method<sup>14</sup> with the measured ionization energies. Since the geometries of all four compounds were not known we have minimized all geometrical parameters of 1–4 with respect to their heats of formation. Another set of calculations

(13) Koopmans, T. *Physica* **1934**, *1*, 104.

(14) Bingham, R. C.; Dewar, M. J. S.; Lo, D. H. *J. Am. Chem. Soc.* **1975**, *97*, 1285. The calculations have been carried out with MOPN:<sup>15</sup> QCPE 1979, 12, 383.

(15) Bischof, P. *J. Am. Chem. Soc.* **1976**, *98*, 6844.

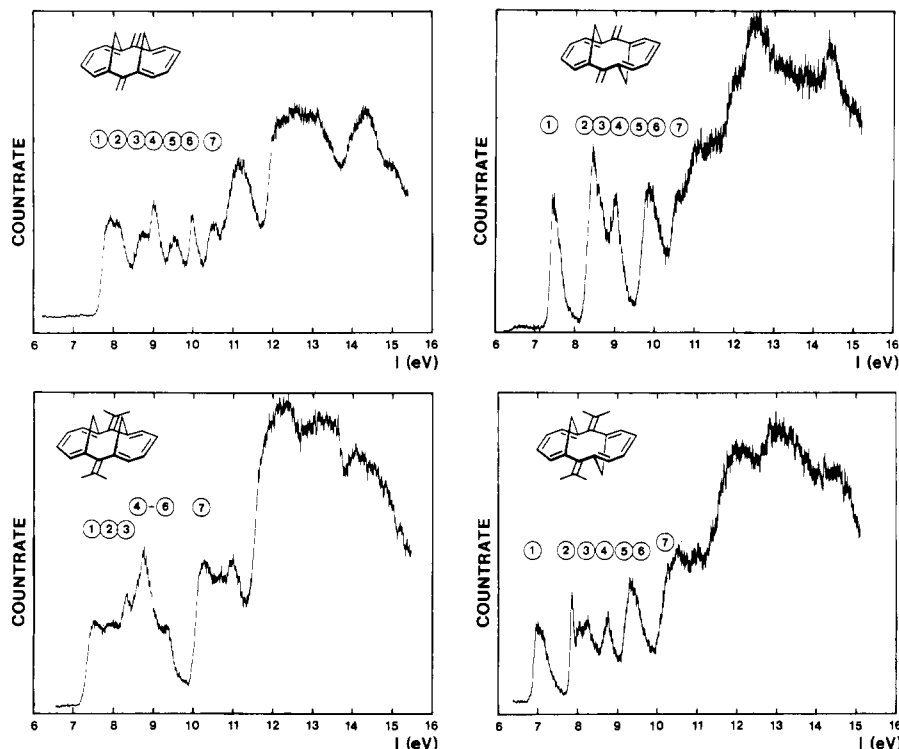


Figure 5. He I $_{\alpha}$  PE spectra of 1-4.

has been carried out by adopting the skeleton of 6 and 7 for 1 and 2 as determined by X-ray investigations and by replacing the two oxygen atoms with methylenes. The resulting orbital energies are very close to those obtained for 1 and 2 by minimizing their geometrical parameters.

To understand the difference in the PE spectra of 1 and 2 and the band pattern which arises from methyl substitution, we start with the MO sequence of 5. The latter compound has been investigated by PE spectroscopy.<sup>16</sup> A comparison between the PE bands and the calculated orbital energies of 5 suggests the sequence  ${}^2B_{1u}$ ,  ${}^2B_{2g}$ ,  ${}^2B_{3g}$ ,  ${}^2A_u$ ,  ${}^2B_{1u}$ , and  ${}^2B_{2g}$  for the first six ionic states. All states are due to ionization from  $\pi$  MOs of 5. The wave functions of the four highest occupied  $\pi$  MOs of 5 are shown in Figure 6. Below each MO is given the irreducible representation of the appropriate point group  $D_{2h}$  (5),  $C_{2v}$  (1, 3), and  $C_{2h}$  (2, 4).

Bridging the centers of 1, 6 and 8, 13 of 5 by methano bridges will have three effects: (i) a reduction of symmetry from  $D_{2h}$  to  $C_{2v}$  (1, 3) and  $C_{2h}$  (2, 4), respectively, (ii) a pronounced bond alternation in both hexatriene units (see Figures 1 and 2), and (iii) a change of the basis orbital energies of the  $\pi$  and  $\sigma$  MOs due to the enlargement of the  $\sigma$  skeleton.

The extension of the  $\sigma$  frame will lead to a destabilization of all MOs by 0.2-0.3 eV. To discuss the consequences of the bond alternation on going from 5 to 1 and 2, respectively, we will use arguments from first-order perturbation theory.<sup>17</sup> A lengthening of bonds C(1)-C(6) and C(8)-C(13) together with the appropriate alternation along the periphery (e.g., shortening of bonds C(1)-C(2), C(3)-C(4), C(5)-C(6), C(8)-C(9), C(10)-C(11), and C(12)-C(13)) will destabilize  $b_{1u}$  and  $b_{3g}$  and stabilize  $b_{2g}$  and  $a_u$ . Due to its nonplanarity and reduced symmetry, the  $\sigma$  frame is no longer orthogonal to the  $\pi$  system and as a consequence  $\pi/\sigma$  mixing occurs. For reasons of symmetry, the  $2b_{2u}$   $\sigma$  MO of 5 ( $D_{2h}$ ) cannot interact with any  $\pi$  MO. When the symmetry is reduced to  $C_{2v}$  or  $C_{2h}$ , however, interaction with the  $\pi$  MOs of  $B_2$  and  $B_u$  symmetry is efficient due to a large overlap of both the  $\pi$  and the

$\sigma$  systems (see Figure 6). As a consequence of this interaction the  $b_2$  and the  $b_u$  MO of 1 and 2 are destabilized considerably. Taking all three changes together, we anticipate the following differences when comparing the four highest occupied MOs of 5 with those of 2: a strong destabilization of  $b_u$ , a moderate destabilization of  $a_g$  and  $a_u$ , and a stabilization of  $b_g$ . The same arguments yield for the comparison 5 with 1 a strong destabilization of  $b_2$ , a moderate destabilization of  $a_1$  and  $a_2$ , and a stabilization of  $b_1$ .

The ionization energies of the first bands of the PE spectra of 1 and 2 are compared with those of 5 in Figure 7. This comparison is based on the MO results given in Table I. The correlation shown is that anticipated from  $\pi/\sigma$  interaction mainly ( $b_{3g}$  and  $b_{1u}$  are destabilized strongly). The expected effects for bond alternation are observed to a minor extent only. The fact that bond alternation has only a minor effect on  $\pi$  levels has been discussed earlier with benzene<sup>11</sup> and pentalene<sup>18</sup> as examples.

To check our assignment of the first PE bands of 1 and 2 we have recorded the PE spectra of the tetramethyl derivatives 3 and 4. With use of first-order perturbation theory<sup>20</sup> as a guide it seems safe to argue that  $\pi$  MOs are shifted by methyl groups proportionally to the square of the size of the  $2p_z$ AO coefficient at the position of substitution. Using these criteria we anticipate that those bands arising from MOs of the irreducible representations  $A_1$ ,  $B_u$  or  $B_1$ ,  $B_g$  (see Figure 6) will be shifted strongly in the tetramethyl derivatives 3 and 4, while the MOs  $b_2$ ,  $a_g$  and  $a_2$ ,  $a_u$  should remain constant due to the node passing through the methylene groups. A comparison between the PE spectra of 1 and 3 as well as 2 and 4 shows, however, an almost equal shifting of all bands due to methyl substitution as can be seen from Figure 8. A more careful examination of the PE spectra of 1 and 2 indicates that the shifts of  $14a_1$  and  $10b_1$  are stronger than those

(18) Gleiter, R.; Bischof, P. In *Topics in Nonbenzenoid Aromatic Chemistry*; Hirokawa Publishing Co.: Tokyo, 1977 Vol. 2, p 1.

(19) Brogli, F.; Clark, P. A.; Heilbronner, E.; Neuenschwander, M. *Angew. Chem.* 1973, 85, 414; *Angew. Chem., Int. Ed. Engl.* 1973, 12, 422. Welsher, T. L.; Buscheck, J. M.; Nelin, C. J.; Matsen, F. A. *Chem. Phys. Lett.* 1979, 67, 479. Koenig, T.; Klopfenstein, C. E.; Southwork, S.; Hoobler, J. A.; Wielek, R. A.; Balle, T.; Smell, W.; Imre, D. J. *Am. Chem. Soc.* 1983, 105, 2256.

(20) Lauer, G.; Schäfer, W.; Schweig, A. *Chem. Phys. Lett.* 1975, 33, 312.

(21) For definition of the  $N$  value, see: Günther, H. *Angew. Chem.* 1972, 84, 907; *Angew. Chem., Int. Ed. Engl.* 1972, 11, 861.

(16) Allan, M.; Heilbronner, E.; Kaupp, G. *Helv. Chim. Acta* 1976, 59, 1949.

(17) Heilbronner, E.; Bock, H. *Das HMO Modell und seine Anwendung*; Verlag Chemie: Weinheim, 1968. Dewar, M. J. S. *The Molecular Orbital Theory of Organic Chemistry*; McGraw Hill: New York, 1969.

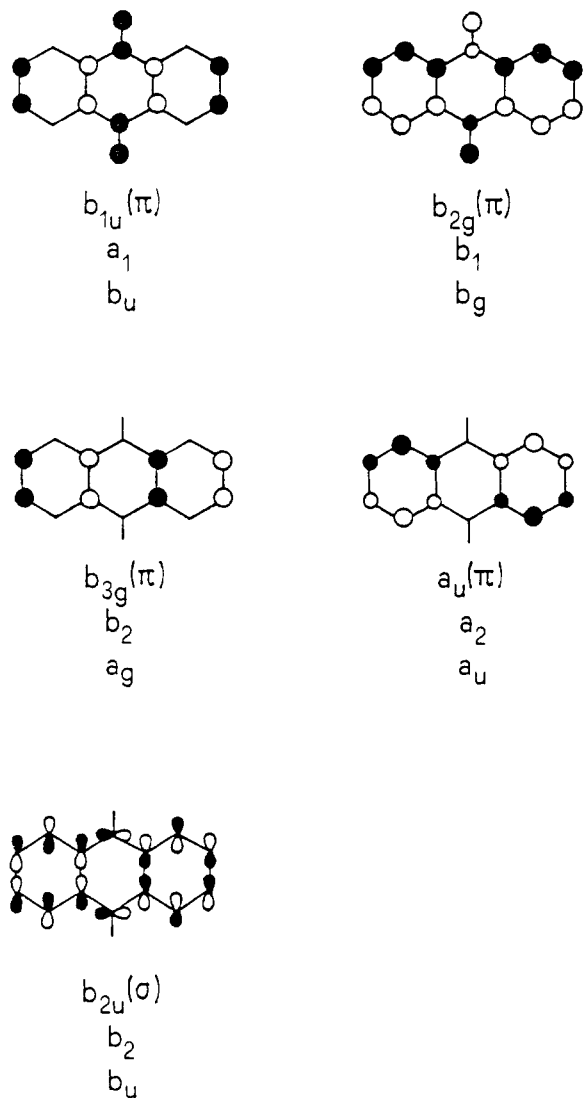


**Figure 6.** Highest occupied and lowest unoccupied MOs of **5**. Below each wave function its irreducible representation in the point group  $D_{2h}$ ,  $C_{2v}$ , and  $C_{2h}$ , respectively, is given.

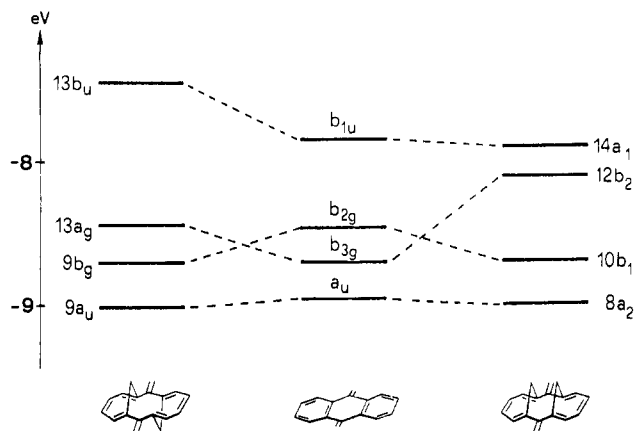


**Figure 7.** Comparison between the highest occupied MOs of **5** (middle) and those of **1** (right) and **2** (left). The energies are taken from PE measurements.

of  $12b_2$  and  $8a_2$ , but it is still not explained satisfactorily. A similar situation has been encountered for fulvene and its methyl derivatives.<sup>19</sup> An analysis of the situation in fulvene<sup>19</sup> shows that for those MOs which are strongly localized in only a part of the molecule, correlation and reorganization effects do not cancel each other any more. For those cases Koopmans' theorem is not valid. In our case the relatively strongly localized MOs are  $b_2$  and  $a_g$

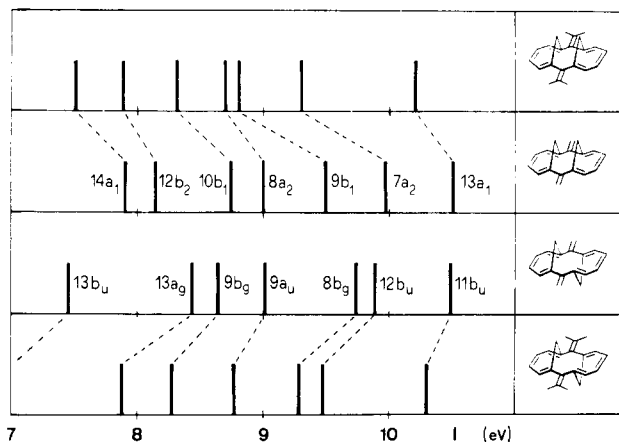


**Figure 8.** Comparison between the first bands in the PE spectra of **1** and **2** and with those of **3** and **4**, respectively.

**Table II.** Comparison between the Vertical Ionization Energies,  $I_{v,j}$ , and the Calculated Orbital Energies,  $\epsilon_j$ , of **6** and **7**<sup>a</sup>

compd	band	$I_{v,j}$	assignment	$-\epsilon_j$ (MINDO/3)
6	1	8.6	$12b_2$ ( $\pi$ )	8.44
	2	8.76	$8a_2$ ( $n$ -)	8.85
	3	9.1	$14a_1$ ( $\pi$ )	8.85
	4		$11b_2$ ( $n$ -)	9.14
	5		$10b_1$ ( $\pi$ )	9.62
	6	10.1	$7a_2$ ( $\pi$ )	10.18
	7	11.1	$10b_2$ ( $\pi$ )	11.05
	8		$13a_1$ ( $\pi$ )	11.25
7	1	8.7	$13b_u$ ( $\pi$ - $n$ -)	8.68
	2		$9b_g$ ( $n$ - $\pi$ )	8.90
	3		$13a_g$ ( $\pi$ )	8.61
	4	9.42	$9a_u$ ( $\pi$ )	9.21
	5	9.7	$12b_u$ ( $n$ -)	9.72
	6	10.14	$8b_g$ ( $\pi$ )	10.20
	7	11.2	$11b_u$ ( $\pi$ )	11.16
	8		$12a_g$ ( $\pi$ )	11.19

<sup>a</sup> The calculations were carried out with the MINDO/3 method. All values in eV.

for **2** and  $a_2$  and  $a_u$  for **1** (see Figure 4). The relaxation process spreads the positive charge also into the region of the system where the orbital density  $\psi_j^2$  is 0. The resultant charge equalization stabilizes the radical cation, and if the molecule is substituted at those positions where  $\psi_j^2 = 0$ , then these substituents will also be included in the stabilization process. Thus the  $CH_3$  groups still donate electron density in the  ${}^2B_2$ ,  ${}^2A_g$ ,  ${}^2A_2$ , and  ${}^2A_u$  states, respectively. As a net effect, we observe in these states larger Koopmans' defects than in the others. From these observations we anticipate similar effects when comparing **5** with the corresponding methyl derivatives.

### PE Spectra of **6** and **7**

In Figure 9 we compare the PE spectra of **6** and **7** with that of anthraquinone (**8**). The difference between the spectra of the bishomoanthraquinones and that of **8** is striking. In the PE spectrum of the latter compound<sup>20</sup> we observe one broad band between 9 and 10 eV, well separated from strongly overlapping bands starting around 11.5 eV. The PE spectra of **6** and **7**, in contrast, show four (6) or five (7) distinct peaks in the area between 8 and 12 eV. Due to the different half-widths of the peaks, we assign eight bands to these peaks as shown in Figure 9. The recorded ionization energies of **6** and **7** are listed in Table II.

To assign the PE spectra of **6** and **7** we will rely mainly on the results of MINDO/3 calculations since the sequence of energy levels obtained by this method corresponds to the band pattern, as far as the highest occupied MOs are concerned (see Tables I and II).

The calculation predicts eight ionic states between 8 and 11.5 eV. Furthermore, the calculation predicts for the energy difference between the first six energy levels of both compounds a value of

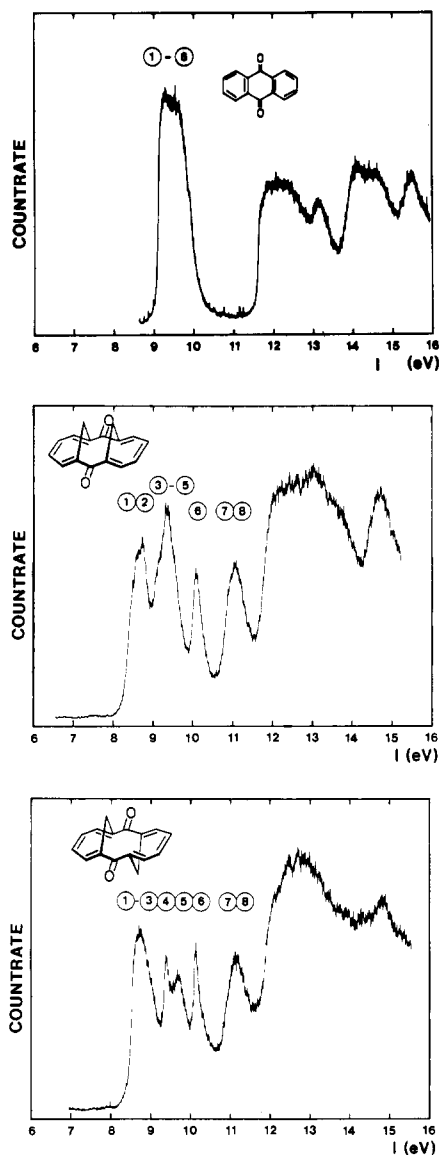


Figure 9. Comparison of the PE spectra of 6 and 7 with that of 8.

1.4 and 1.5 eV, respectively, which is close to the half-width of the first six bands (see Figure 9).

On the basis of the results of 1-5 it seems reasonable to assume that the main difference between the first six bands in the PE spectrum of 8 on the one side and 6 and 7 on the other side is due to  $\pi/\sigma$  interaction. This assumption is supported by the result that in 6-8 there are two high-lying  $\sigma$  orbitals,  $b_{1g}(n_-)$  and  $b_{2u}(n_+)$ . To discuss the possibilities of  $\pi/\sigma$  interaction in 6 and 7 we consider in Figure 10 the six highest occupied MOs of 8. Below each drawing the irreducible representation in the point groups  $D_{2h}$  (8),  $C_{2v}$  (6), and  $C_{2h}$  (7) are given. From this figure it is evident that the reduction of symmetry from  $D_{2h}$  to  $C_{2v}$  and  $C_{2h}$ , respectively, will allow a mixing between  $n_-$  and  $n_+$  with the corresponding  $\pi$  MOs. Since the energy levels of all six MOs are very close together, and since a sizable overlap is inferred from the coefficients, we expect a strong  $\pi/\sigma$  interaction between  $a_2(n_-)$  and  $a_2(\pi)$  as well as  $b_2(n_+)$  and  $b_2(\pi)$  for 6 and  $b_g(n_-)$  and  $b_g(\pi)$  as well as  $b_u(n_+)$  and  $b_u(\pi)$  for 7. These qualitative arguments are supported by the PE spectra in so far as in 6 and 7 the half-width of the first bands is double (ca. 1.6 eV) compared with that in 8 (ca. 0.8 eV).

A correlation between the PE bands of 8 with those of 6 and 7 is hampered by the fact that the sequence of the bands in 8 cannot be determined unequivocally due to the strong overlap of all six bands. In adopting the assignment for 6 and 7 given in Table II, we can rationalize the splitting pattern observed by assuming the following sequence for 8:  ${}^2B_{3g}$ ,  ${}^2B_{1g}$ ,  ${}^2B_{1u}$ ,  ${}^2B_{2u}$ ,  ${}^2B_{2g}$ ,

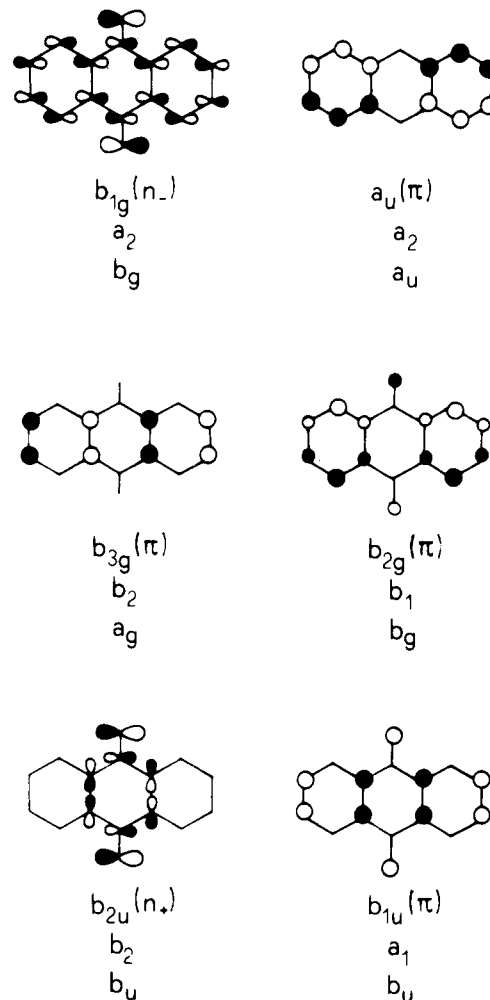


Figure 10. Schematic drawing of the six highest occupied MOs of 8. Below each wave function its irreducible representation in the point group  $D_{2h}$ ,  $C_{2v}$ , and  $C_{2h}$ , respectively, is given.

and  ${}^2A_u$ . In Figure 11 we have correlated the first six states of 6 and 7 with those of 8. Our correlation with the bands of 8 (center) and the adopted sequence of the PE bands in this molecule is based on the following assumptions. (i) Those MOs which have no partner to interact with when reducing symmetry ( $b_1$ ,  $a_1$  and  $a_u$ ,  $a_g$ ) should be destabilized by about 0.4 eV due to the  $\text{CH}_2$  bridges. (ii) The main reason for the strong split of the half-widths is due to  $\pi/\sigma$  interaction when reducing the symmetry from  $D_{2h}$  (8) to  $C_{2v}$  (6) or  $C_{2h}$  (7).

The assignment obtained for the first six bands of 8 by this correlation differs from that tentatively proposed by Schweig et al.<sup>20</sup> in so far as we suggest that the HOMO is a  $\pi$  orbital and not  $n_-$ . Our assignment agrees with that proposed in so far as the lone-pair splitting in 8 does not exceed 0.3 eV.

#### Concluding Remarks

By comparing the sequence of the highest occupied MOs of the nonplanar species 1-4 and 6 and 7 with its planar congeners (5 and 8, respectively) we have demonstrated not only that  $\pi/\sigma$  interaction can be large but that the effect of  $\pi/\sigma$  interaction leads to a destabilization of  $\pi$  orbitals in the order of 0.2 to 0.8 eV in the case of the hydrocarbons and up to 1.3 eV in the case of the carbonyl compounds. This is the first quantitative assessment of these effects.

Our calculations, together with the PE spectroscopic investigations, even suggest that the HOMO in 7 has a different shape than that in 6 and 8. In the case of reactions in which the HOMO mainly determines the selectivity, we thus expect differences between 7 on one side and 6 and 8 on the other.

It is further worthwhile mentioning that the  $\pi/\sigma$  interaction also affects the LUMO. Recently, we have demonstrated by

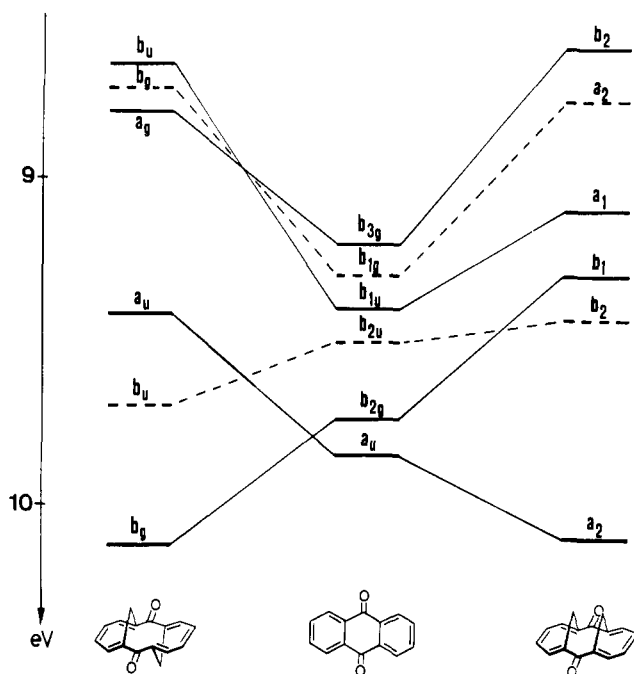


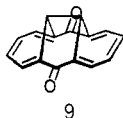
**Figure 11.** Comparison between the highest occupied MOs of 8 (middle) and its nonplanar congeners 6 (right) and 7 (left). The energies for the bands of 6 and 7 are taken from PE experiments.  $\pi$  bands are indicated by solid lines and n bands by broken ones.

means of cyclic voltammetry<sup>9d</sup> that the difference of the reduction potentials ( $E_2 - E_1$ ) between 6, 7, and 8 can be explained by a larger delocalization of the unpaired electron in 6<sup>-</sup> and 7<sup>-</sup> compared with 8<sup>-</sup>. This larger delocalization is caused by  $\pi/\sigma$  interaction.

Our studies allow us also to suggest a consistent interpretation for the first six ionic states of anthraquinone (see Figure 11). The suggested orbital sequence is in line with Green's function calculations on 8. These calculations indicate that, although the Koopmans' defects differ for  $\pi$  and  $\sigma$  levels, a crossing does not occur. Thus the assumption of the validity of Koopmans' theorem is reasonable.

Since our calculations carried out on 1-8 parallel very well the PE results, the following corollaries, derived from MINDO/3 calculations, are likely:

(1) The bridged bishomoanthraquinone (9) should be an interesting target to synthesize because it is predicted to be flatter



than 6 and thus we expect a reduced  $\pi/\sigma$  interaction. A study of its PE spectrum should yield the result that the widths of the first six bands of 9 are intermediate between the widths of 6 and 8. Furthermore, the difference in its reduction potentials ( $E_2 - E_1$ ) should also be in between that of 6 and 8.

(2) As a consequence of the very strong  $\pi/\sigma$  interaction in 6 and 7 the calculations predict a strong rotation of the  $p_x$  atomic orbitals (AOs) of the highest occupied MOs. In the HOMO of 6 the  $p_x$  AOs at the peripheral centers (2-5 and 9-12) are rotated away from the methano bridges. If an electrophile approaches the carbon skeleton, the approach at these positions should occur from the side syn to the methano bridges. A similar stereoselectivity has been observed for 1,6-methano[10]annulene.<sup>22</sup>

## Experimental Section

**Spectroscopic and X-ray Investigations.** The PE spectra of 1-4, 6, 7, and 8 were recorded on a UPS-200 from Leybold Heraeus and on a PS18

**Table III.** Crystallographic Data and Refinement Parameters of 6 and 7

	6	7
crystal system	orthorhombic	monoclinic
space group	<i>Pca</i> 2 <sub>1</sub>	<i>C2/c</i>
Z	16	4
a, Å	14.051 (1)	9.194 (2)
b, Å	9.439 (1)	8.687 (2)
c, Å	35.881 (1)	14.581 (3)
$\beta$ , deg		91.30 (2)
crystal size [mm <sup>3</sup> ]	0.5 × 0.4 × 0.4	0.3 × 0.3 × 0.25
reflcs collected	4945	4010
unique reflcs	4945	1696
obsd reflcs	4021	1269
refinement	0.044/0.068	0.047/0.048
$R/R_w$ <sup>a</sup>		
max heights of diff synth, e Å <sup>-3</sup>	0.17	0.36

$$w = \{[\sum w(|F_o| - |F_c|)^2] / [\sum w F_o^2]\}^{1/2}; w = 1/\sigma^2(F_o).$$

from Perkin Elmer. The calibration was carried out with Ar and Xe. A resolution of 0.03 eV is found for the sharp peaks. For the X-ray analysis, the yellow crystals of 6 and the colorless crystals of 7 were grown from methylene chloride and ethyl acetate, respectively. The crystallographic data and the parameters of structure refinement are listed in Table III. The data were collected on an automatic diffractometer (Enraf-Nonius CAD-4, Mo K $\alpha$  radiation, graphite monochromator,  $2\theta-\omega$  scanning). The solutions of the structures with direct methods and the refinements in full-matrix technique of  $F^2$  were carried out with the SHELX program system.

**Preparation of 1-4.** Melting points are uncorrected. Chemical shifts are reported in parts per million downfield from tetramethylsilane as internal standard for <sup>1</sup>H and <sup>13</sup>C NMR spectra.

**7,14-Dimethylene-7,14-dihydro-syn-1,6:8,13-bismethano[14]annulene (1).** To a suspension of 1.43 g (4 mmol) of methyltriphenylphosphonium bromide in 20 mL of dry THF is added dropwise 2 mL (4 mmol) of a 2 M solution of *n*-butyllithium in *n*-hexane. After 30 min of stirring, the ylide solution is added within 10 min to a solution of 236 mg (1 mmol) of the syn-diketone 6 in 20 mL of THF. After refluxing for 15 min the solution is filtered through Al<sub>2</sub>O<sub>3</sub> (Brockmann) and extracted with CH<sub>2</sub>Cl<sub>2</sub>. The solvent is removed and the solution of the residue in *n*-pentane is chromatographed on Al<sub>2</sub>O<sub>3</sub> (Brockmann, 15/3 cm). Removal of the solvent yields 206 mg (89%) of a yellow oil. Colorless crystals are obtained from *n*-pentane at low temperature, mp 105-106 °C. <sup>1</sup>H NMR (300 MHz, CDCl<sub>3</sub>):  $\delta$  6.48 and 6.14 (AA'BB',  $N^{21} = 5.9$  Hz, 8 H), 5.17 (s, 4 H), 4.10 and 1.68 (AX,  $^2J = -12.64$  Hz, 4 H). <sup>13</sup>C NMR (75.5 MHz, CDCl<sub>3</sub>):  $\delta$  152.05 (s, C-7,14), 138.40 (s, C-1,6,8,13), 128.63 (d, C-3,4,10,11), 121.71 (d, C-2,5,9,12), 110.03 (t, C-17,18), 34.91 (t, C-15,16). MS (70 eV):  $m/z$  232 (M<sup>+</sup>, 100%), 215 (91), 202 (98). IR (KBr): 1605 cm<sup>-1</sup> (C=C). UV/VIS (dioxane):  $\lambda_{max} = 232$  nm ( $\epsilon$  32400), 281 (9800). Calcd for C<sub>18</sub>H<sub>16</sub> 232.1252, found  $m/z$  232.1246.

**7,14-Dimethylene-7,14-dihydro-anti-1,6:8,13-bismethano[14]annulene (2).** To a solution of 236 mg (1 mmol) of 7 in 100 mL of dry THF at room temperature 2.25 mmol of methylolithium in ether is added dropwise. After 2 h of stirring the solution is poured into 10 mL of ice-water. This mixture is poured under ice-cooling into a solution of 10 mL of H<sub>2</sub>SO<sub>4</sub> in 20 mL of H<sub>2</sub>O and stirred for 0.5 h. After extraction (3 times) with ether, the organic solvents are washed with saturated NaHCO<sub>3</sub> solution and H<sub>2</sub>O, dried (MgSO<sub>4</sub>), and evaporated. The residue is dissolved in *n*-hexane/dichloromethane (1:1) and chromatographed on silica gel (15/3 cm). The first fraction yields 190 mg (82%) of 2. Recrystallization from methanol gives pale yellow needles, mp 142-143 °C. <sup>1</sup>H NMR (300 MHz, CDCl<sub>3</sub>):  $\delta$  6.60 and 6.42 (AA'BB',  $N^{21} = 6.1$  Hz, 8 H), 5.28 (s, 4 H), 2.82 and 1.71 (AX,  $^2J = -12.64$  Hz, 4 H). <sup>13</sup>C NMR (75.5 MHz, CDCl<sub>3</sub>):  $\delta$  153.29 (s, C-7,14), 137.72 (s, C-1,6,8,13), 130.22 (d, C-3,4,10,11), 123.65 (d, C-2,5,9,12), 109.02 (t, C-17,18), 34.56 (t, C-15,16). MS (70 eV):  $m/z$  232 (M<sup>+</sup>, 100%), 215 (65), 202 (76). IR (KBr): 1596 cm<sup>-1</sup> (C=C). UV/VIS (dioxane):  $\lambda_{max} = 231$  nm ( $\epsilon$  42200), 307 (11500). Calcd for C<sub>18</sub>H<sub>16</sub> 232.1252, found  $m/z$  232.1256.

**7,14-Disopropylidene-7,14-dihydro-syn-1,6:8,13-bismethano[14]annulene (3).** To 2.31 g (6 mmol) of powdered and dried isopropyltriphenylphosphonium bromide a solution of 672 mg (6 mmol) of freshly sublimed potassium *tert*-butylate in 8 mL of dry Me<sub>2</sub>SO is added dropwise. After the mixture is stirred for 30 min a solution of 236 mg (1 mmol) of the syn-diketone 6 in a small amount of Me<sub>2</sub>SO is added to the ylide solution. The dark-violet mixture is stirred at 65 °C for 1 h. After cooling the solution is hydrolyzed with 50 mL of H<sub>2</sub>O, followed by extraction with *n*-hexane. The organic solvent is dried (MgSO<sub>4</sub>) and removed. The residue is chromatographed on silica gel (15/3 cm) in

(22) Gleiter, R.; Böhm, M. C.; Vogel, E. *Angew. Chem.* 1982, 94, 925; *Angew. Chem., Int. Ed. Engl.* 1982, 21, 922.

*n*-hexane/dichloromethane (1:1). The first fraction yields after evaporation of the solvent 180 mg (63%) of colorless **3**. Recrystallization from methanol affords colorless needles, mp 148–149 °C. <sup>1</sup>H NMR (300 MHz, CDCl<sub>3</sub>): δ 6.34 and 5.73 (AA'BB', *N*<sup>21</sup> = 5.9 Hz, 8 H), 3.64 and 2.05 (AX, <sup>2</sup>*J* = -12.2 Hz, 4 H), 1.87 (s, 12 H). <sup>13</sup>C NMR (75.5 MHz, CDCl<sub>3</sub>): δ 143.25 (s, C-1,6,8,13), 138.88 (s, C-7,14), 127.67 (d, C-3,4,10,11), 125.57 (s, C-17,18), 121.98 (d, C-2,5,9,12), 38.74 (t, C-15,16), 21.43 (q, C-19,20,21,22). MS (70 eV): *m/z* 288 (M<sup>+</sup>, 98%), 273 (9), 258 (10), 115 (100). IR (KBr): 1607 cm<sup>-1</sup> (C=C). UV/VIS (dioxane): λ<sub>max</sub> = 230 nm (ε 28 800), 258 (8000), 287 (6300). Anal. Calcd for C<sub>22</sub>H<sub>24</sub> (288.4): C, 91.61; H, 8.39. Found: C, 91.82; H, 8.26.

**7,14-Diisopropylidene-7,14-dihydro-anti-1,6:8,13-bismethano[14]-annulene (4)**. To a solution of 236 mg (1 mmol) of the anti-diketone **7** in 100 mL of dry THF are added 5 mmol of isopropylmagnesium bromide in 3 mL of ether. After being stirred for 2 h at room temperature the mixture is hydrolyzed with 10 mL of H<sub>2</sub>O under ice-cooling. The mixture is poured into dilute H<sub>2</sub>SO<sub>4</sub> (ice-cooling) prepared from 10 mL of H<sub>2</sub>SO<sub>4</sub> and 20 mL of H<sub>2</sub>O, and stirring is continued for 0.5 h. The solution is extracted three times with 50 mL of ether. After washing (water, sodiumbicarbonate solution) the ethereal solution is dried (MgSO<sub>4</sub>). After evaporation of the solvent, the residue is dissolved in *n*-hexane/dichloromethane (1:1) and chromatographed on silica gel (15/3

cm). The first fraction yields 70 mg (24%) of yellow **4**. Recrystallization from methanol yielded yellow crystals, mp 192–193 °C. <sup>1</sup>H NMR (300 MHz, CDCl<sub>3</sub>): δ 6.52 and 6.15 (AA'BB', *N*<sup>21</sup> = 6.2 Hz, 8 H), 2.75 and 1.92 (AX, <sup>2</sup>*J* = -12.6 Hz, 4 H), 2.05 (s, 12 H). <sup>13</sup>C NMR (75.5 MHz, CDCl<sub>3</sub>): δ 139.99 (s, C-7,14), 138.95 (s, C-1,6,8,13), 131.25 (s, C-17,18), 129.31 (d, C-3,4,10,11), 127.43 (d, C-2,5,9,12), 35.32 (t, C-15,16), 24.89 (q, C-19,20,21,22). MS (70 eV): *m/z* 288 (M<sup>+</sup>, 18%), 273 (1), 258 (3), 91 (100). IR (KBr): 1599 cm<sup>-1</sup> (C=C). UV/VIS (dioxane): λ<sub>max</sub> = 228 nm (ε 33 100), 265 (10 100), 325 (12 300). Anal. Calcd for C<sub>22</sub>H<sub>24</sub> (288.4): C, 91.61; H, 8.39. Found: C, 91.74; H, 8.36.

**Acknowledgment.** We are grateful to the Deutsche Forschungsgemeinschaft, the Fonds der Chemischen Industrie, and the BASF Aktiengesellschaft in Ludwigshafen for financial support. Thanks are due to Alexander Flatow for recording the PE spectra.

**Supplementary Material Available:** Tables of atomic coordinates with standard deviations, bond lengths, bond angles, and torsional angles of **6** and **7** (10 pages). Ordering information is given on any current masthead page.

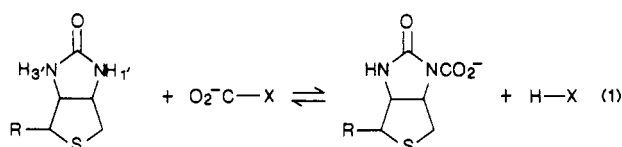
## Proton Exchange in Biotin: A Reinvestigation, with Implications for the Mechanism of CO<sub>2</sub> Transfer

Charles L. Perrin\* and Tammy J. Dwyer

Contribution from the Department of Chemistry, D-006, University of California, San Diego, La Jolla, California 92093. Received February 9, 1987

**Abstract:** Kinetics of proton exchange of biotin and its methyl ester were studied in aqueous buffers. Rate constants were determined by NMR saturation-transfer or line-broadening methods. The reaction was observed to be simply first order in H<sup>+</sup> or OH<sup>-</sup>, in disagreement with a previous study (Fry, Fox, Lane, Mildvan *J. Am. Chem. Soc.* **1985**, *107*, 7659). The mechanisms of proton exchange and the implications for the mechanism of biotin-mediated CO<sub>2</sub> transfer are discussed.

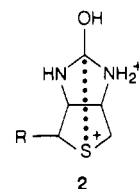
The mechanisms of CO<sub>2</sub> metabolism mediated by biotin (**1**) continue to generate interest.<sup>1</sup> The general reaction is of the form of eq 1 or its reverse, where X = CH<sub>2</sub>CO<sub>2</sub><sup>-</sup> or CH(CH<sub>3</sub>)COSC<sub>2</sub>A.



1: R = HOCO(CH<sub>2</sub>)<sub>4</sub>

Recent results<sup>2</sup> show that X = OPO<sub>3</sub>H<sup>-</sup> also fits this equation, rather than alternatives involving phosphorylated biotin. Many questions have arisen over the details of the C–X and H–X bond-breaking/making steps: What is the timing of those steps? Might the base that removes the proton of HX be biotin?<sup>3</sup> Might that base be the conjugate base of biotin, formed by removal of the 3' proton?<sup>4</sup> Although recent results<sup>5</sup> show that C–X and H–X

bond breaking/making occur stepwise, rather than concerted,<sup>3</sup> similar questions may be raised regarding the breaking of the N–H bond and the formation of the N–C bond. In an attempt to answer these questions, Fry, Fox, Lane, and Mildvan<sup>6</sup> (FFL&M) have studied the kinetics of NH proton exchange in biotin and some of its analogues. All of these show a normal base-catalyzed exchange, first order in OH<sup>-</sup>. Most of them also show a normal acid-catalyzed exchange, first order in H<sup>+</sup>. However, biotin itself and its methyl ester were found to undergo an exchange of the 1'NH that is second order in H<sup>+</sup> (Figure 1), even though exchange of the 3'NH is normal. They attributed this exchange to a transannular interaction with the sulfur, which stabilizes the diprotonated intermediate (**2**: R = HOCO(CH<sub>2</sub>)<sub>4</sub> or CH<sub>3</sub>OCO(CH<sub>2</sub>)<sub>4</sub>). However, X-ray and NMR studies<sup>7</sup> on complexes of



biotin with Lewis acids show no evidence for such interaction. Also, kinetic isotope effects<sup>5c</sup> are inconsistent with transannular C–S bonding. Since the second-order exchange (as well as intermediate **2**, plausible only in superacid<sup>8</sup>) is so unprecedented,

(1) Attwood, P. V.; Keech, D. B. *Curr. Top. Cell. Regul.* **1984**, *23*, 1. Dugas, H.; Penney, C. *Bioorganic Chemistry: A Chemical Approach to Enzyme Action*; Springer: New York, 1981; pp 458–477. Wood, H. G.; Barden, R. E. *Annu. Rev. Biochem.* **1977**, *46*, 385.

(2) Hansen, D. E.; Knowles, J. R. *J. Am. Chem. Soc.* **1985**, *107*, 8304. (3) Retej, J.; Lynen, F. *Biochem. Z.* **1965**, *342*, 256. Arigoni, D.; Lynen, F.; Retej, J. *Helv. Chim. Acta* **1966**, *49*, 311.

(4) Fung, C. H.; Gupta, R. K.; Mildvan, A. S. *Biochemistry* **1976**, *15*, 85. Goodall, G. J.; Prager, R.; Wallace, J. C.; Keech, D. B. *FEBS Lett.* **1983**, *163*, 6.

(5) (a) Stubbe, J.; Fish, S.; Abeles, R. H. *J. Biol. Chem.* **1980**, *255*, 236. (b) O'Keefe, S. J.; Knowles, J. R. *J. Am. Chem. Soc.* **1986**, *108*, 328. O'Keefe, S. J.; Knowles, J. R. *Biochemistry* **1986**, *25*, 6077. (c) Attwood, P. V.; Tipton, P. A.; Cleland, W. W. *Ibid.* **1986**, *25*, 8197.

(6) Fry, D. C.; Fox, T. L.; Lane, M. D.; Mildvan, A. S. *J. Am. Chem. Soc.* **1985**, *107*, 7659.

(7) Berkessel, A.; Breslow, R. *Bioorg. Chem.* **1986**, *14*, 249.